Electronic Supplementary Material (ESI) for New Journal of Chemistry.

Solar Light Motivated Photoelectrocatalytic and Photocatalytic Applications Based on Flower-like NV-g-C_3N_5@VS_2 Heterojunction

Bicheng Hu[a], Yuhui Zhang[a], Jincheng Zhang[a], Jiazan Liu[a], Meng Lei[a], Chenxi Zhao[a], Qiujun Lu[a], Haiyan Wang[a]*, Fuyou Du[a]* and Shiying Zhang[b]*

[a] *College of Biological and Chemical Engineering, Changsha University, Changsha, 410022, Hunan Province, China*

[b] *Hunan Key Laboratory of Applied Environmental Photocatalysis, Changsha University, Changsha, 410022, Hunan Province, China*

[c] *Hunan Engineering Research Center of Degradable Materials and Molding Technology, Changsha University, Changsha, 410022, Hunan Province, China*

* Corresponding author; Tel: +86-84261506; Fax: +86-731-84261382;

E-mail address: wanghaiyan@ccsu.edu.cn (Haiyan Wang), dufu2005@126.com (Fuyou Du), cdzhangshiying@163.com (Shiying Zhang)

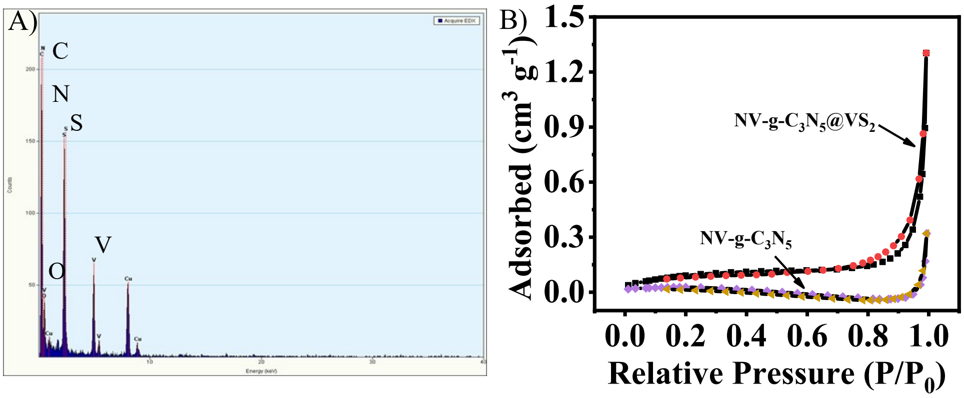

Fig. S1 (A) EDX image of NV-g-C_3N_5@VS_2 heterojunction; (B) N_2 adsorption and desorption isotherm curves of NV-g-C_3N_5 and NV-g-C_3N_5@VS_2 heterojunction.

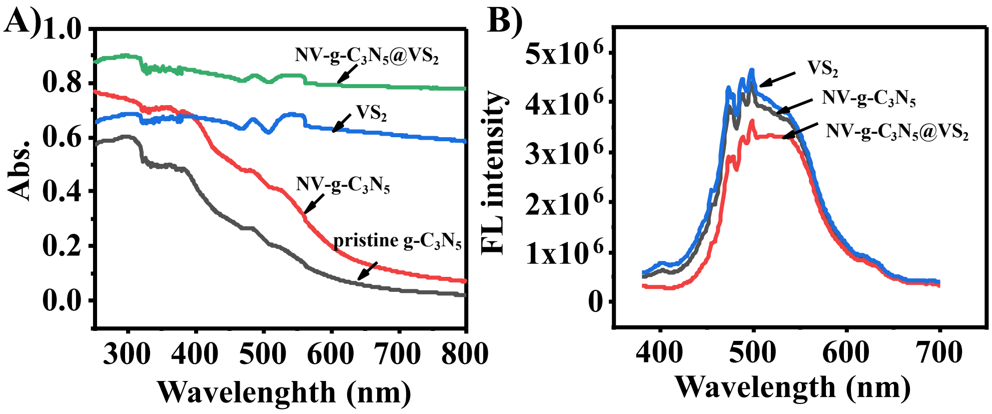

Fig. S2 (A) UV−vis DRS spectra of VS_2, NV-g-C_3N_5, g-C_3N_5 and NV-g-C_3N_5@VS_2 heterojunction. (B) Solid-state fluorescence spectra of VS_2, NV-g-C_3N_5, NV-g-C_3N_5@VS_2.

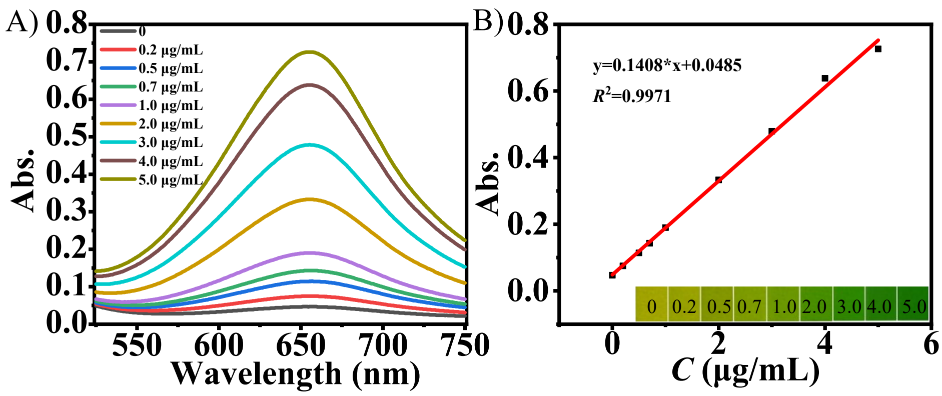

Fig. S3 (A) UV-Vis absorption spectra of NH_4^+ treated with indoxyl blue at room temperature for 2 h. (B) The linear relationship between the standard concentration of NH_4^+ and the absorbance at 650 nm.

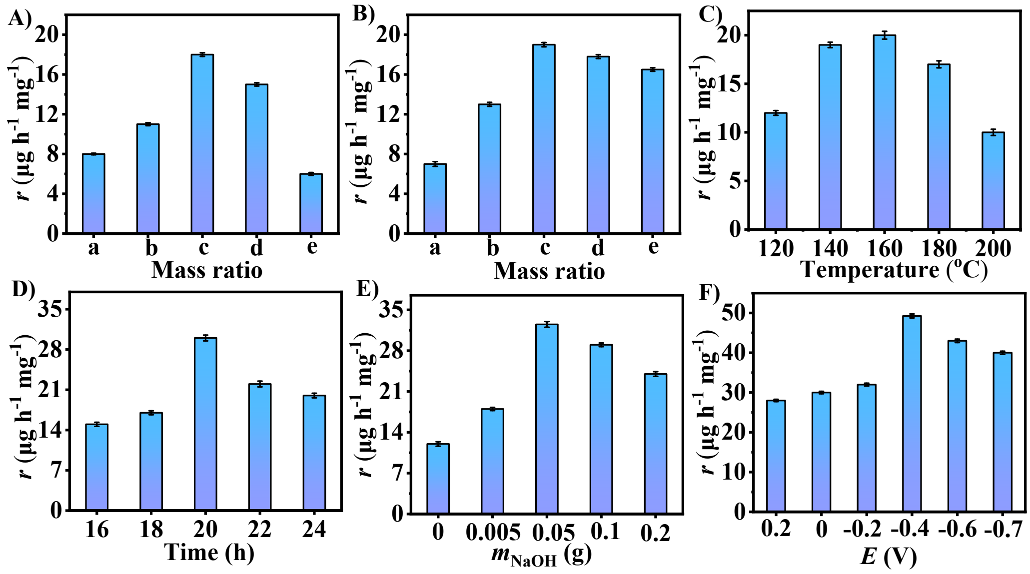

Fig. S4 (A) Ammonia yields of NV-g-C_3N_5@VS_2 heterojunctions synthesized by different mass ratio of NV-g-C_3N_5, ammonium metavanadate and thioacetamide. a, b, c, d and e represent 0.4:0.2:0.8, 0.2:0.2:0.8, 0.1:0.2:0.8, 0.05:0.2:0.8 and 0.04:0.2:0.8, respectively. (B) Ammonia yields of NV-g-C_3N_5@VS_2 heterojunctions synthesized by different mass ratio of NV-g-C_3N_5, ammonium metavanadate and thioacetamide. a, b, c, d and e represent 0.1:0.2:0.2, 0.1:0.2:0.4, 0.1:0.2:0.6, 0.1:0.2:0.8 and 0.1:0.2:1.0, respectively. (C) Ammonia yields of NV-g-C_3N_5@VS_2 heterojunctions synthesized by different hydrothermal temperature. (D) Ammonia yields of NV-g-C_3N_5@VS_2 heterojunctions synthesized by different hydrothermal time. (E) Ammonia yields of NV-g-C_3N_5@VS_2 heterojunctions synthesized by NV-g-C_3N_5 treated with different NaOH (0, 0.005, 0.05, 0.1, 0.2, 0.3 g). (F) Ammonia production rates of NV-g-C_3N_5@VS_2 heterojunctions catalyzed at different applied voltages for 1 h.

Tab. S1 Comparison of photoelectric catalytic nitrogen reduction with different materials.

Material	electrolyte solution	Ammonia production rate（μg h^{-1} mg^{-1}）	References
NV-g-C_3N_5/BiOBr	0.05 M HCl+0.05 M Na_2SO_4	29.4	[1]
N-NiO/CC	0.1 M $LiClO_4$ at −0.5 V	22.7	[2]
Au NPs-PTFE	0.05 M H_2SO_4+0.05 M Na_2SO_3	18.9	[3]
g-C_3N_4 /ZnMoCdS	0.1 M KCl	2.5	[4]
Au/TiO_2	0.1 M HCl at −0.40 V	34.1	[5]
NV-g-C_3N_5/VS_2	0.1 M Na_2SO_4	49.26	This work

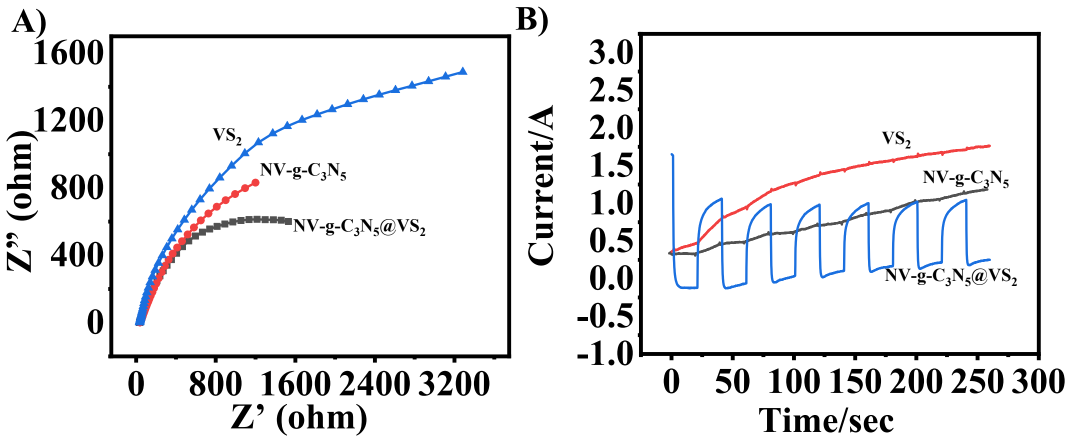

Fig. S5 (A) The electrochemical impedance spectroscopy (EIS) results and (B) photocurrent responses of NV-C_3N_5, VS_2 and NV-g-C_3N_5@VS_2 heterojunction under visible light irradiation, respectively.

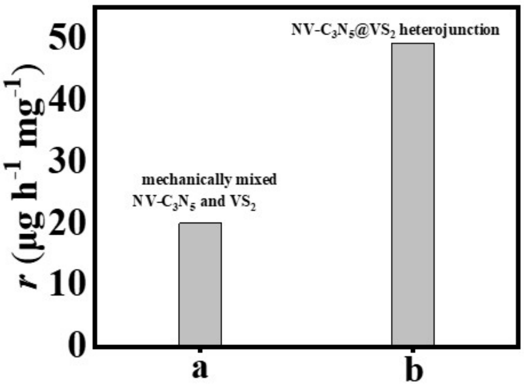

Fig. S6 The productive rate of ammonia of the mechanically mixed NV-C_3N_5 and VS_2 (a), and NV-g-C_3N_5@VS_2 heterojunction (b) in 0.1 M Na_2SO_4 solution filled N_2 with the bias voltage of -0.4 V under visible light.

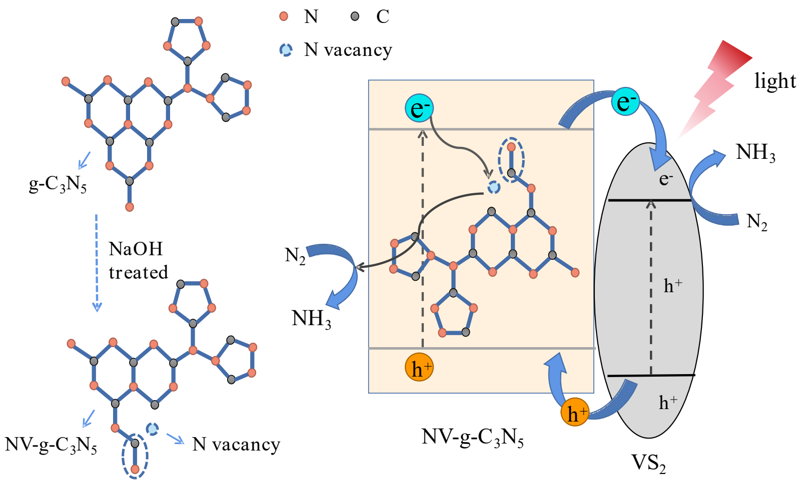

Fig. S7 Schematic illustration of the preparation of NV-g-C_3N_5 and the photoelectric catalytic nitrogen reduction reaction of NV-g-C_3N_5@VS_2 heterojunction.

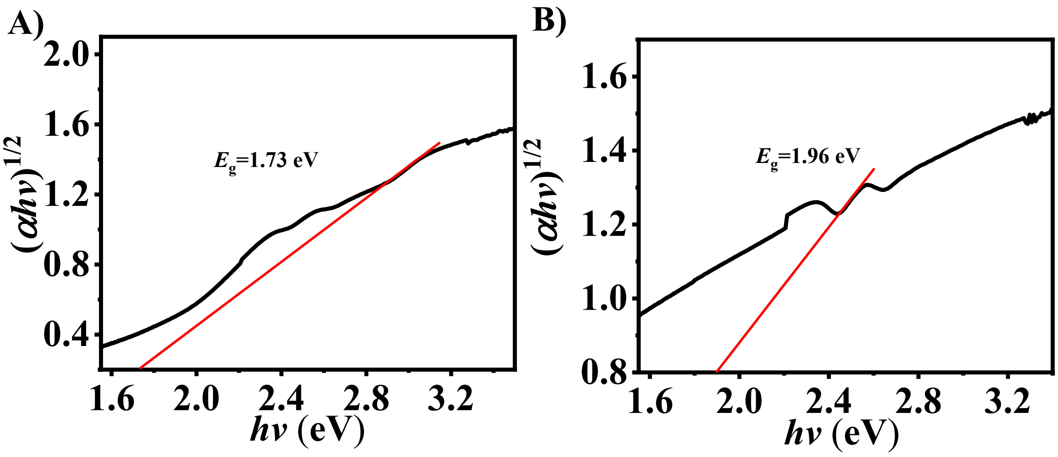

Fig. S8 Plots of transformed Kubelka–Munk function versus photon energy of (A) NV-g-C_3N_5 and (B) VS_2.

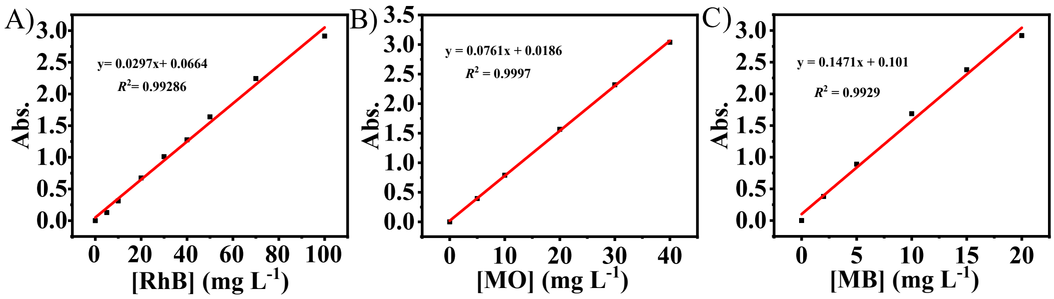

Fig. S9 The linear relationships between the absorbance and the standard concentration of RhB MB and MO, respectively.

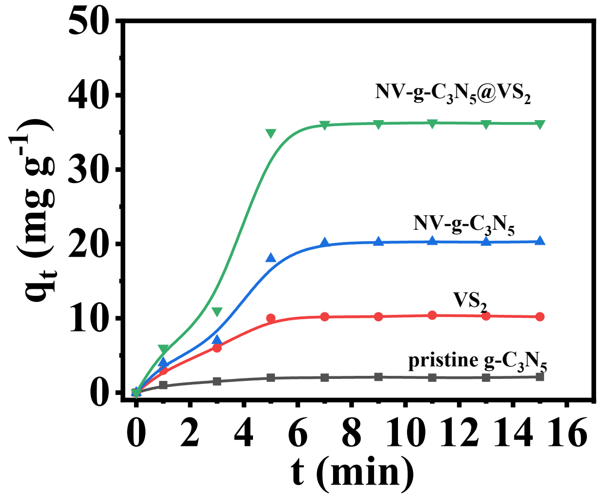

Fig. S10 The maximum adsorption capacity of pristine g-C_3N_5, NV-g-C_3N_5, VS_2 and NV-g-C_3N_5@VS_2 heterojunction.

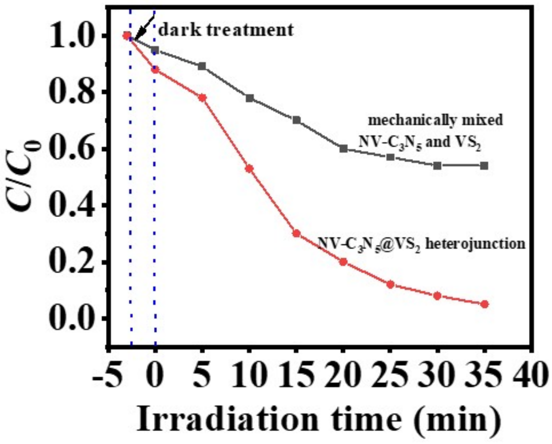

Fig. S11 The changes ratio Rhodamine concentration with irradiation time over the mechanically mixed NV-C_3N_5 and VS_2 (a), and NV-g-C_3N_5@VS_2 heterojunction under visible light irradiation. C_0=40 mg L^{-1}.

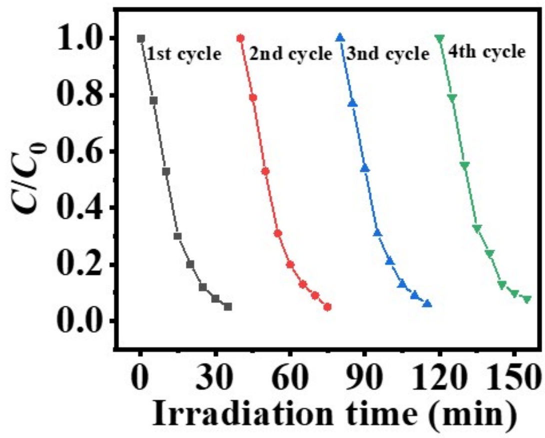

Fig. S12 Recyclability of the visible photocatalytic decomposition of MB by NV-g-C_3N_5@VS_2 heterojunction. C_0 is the initial concentration of RB. C is the remaining concentration of RB. C_0=40 mg L^{-1}.

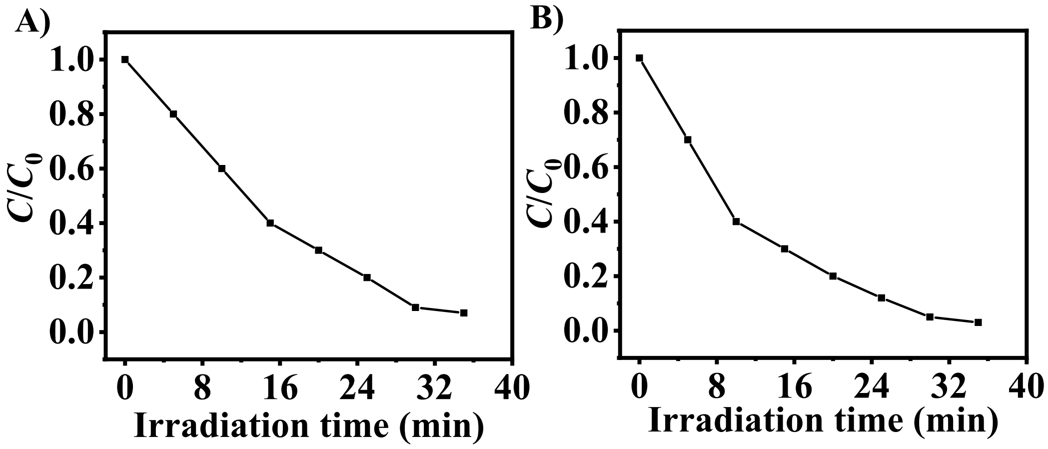

Fig. S13 The change ratio (A) MO and (B) MB concentration with irradiation time over NV-g-C_3N_5@VS_2 heterojunction under visible light irradiation. C_0=40 mg L^{-1}. C_0 and C are the original and the remaining concentration of pollution (MO and MB), respectively.

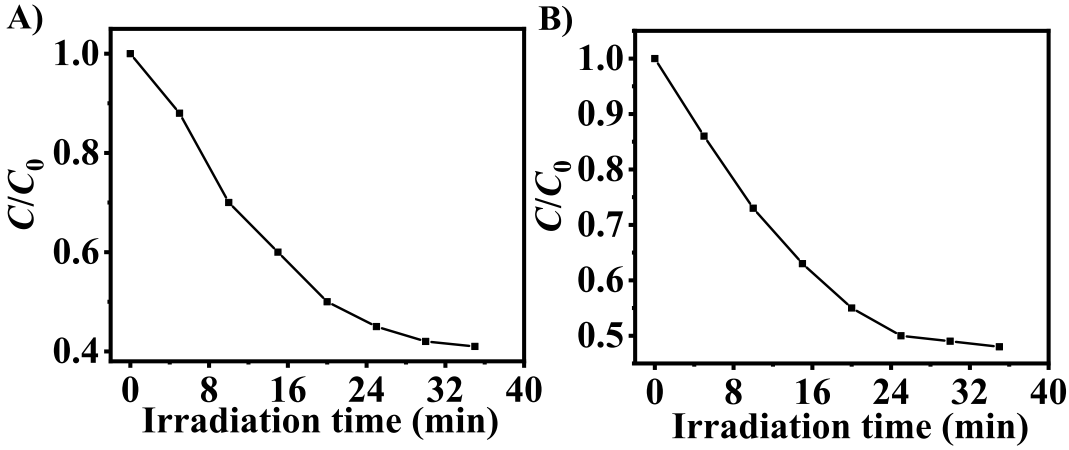

Fig. S14 The changes ratio RB concentration with (A) p-benzoquinone and (B) dimethyl sulfoxide over NV-g-C_3N_5@VS_2 heterojunction under visible light irradiation.

Reference

1. Li, M.; Lu, Q.; Liu, M.; Yin, P.; Wu, C.; Li, H.; Zhang, Y.; Yao, S., Photoinduced charge separation via the double-electron transfer mechanism in nitrogen vacancies g-C_3N_5/BiOBr for the photoelectrochemical nitrogen reduction. *ACS Appl. Mater. Inter.* **2020,** *12* (34), 38266-38274.
2. Wang, X.-h.; Wang, J.; Li, Y.-b.; Chu, K., Nitrogen-doped NiO nanosheet array for boosted electrocatalytic N_2 reduction. *ChemCatChem* **2019,** *11* (18), 4529-4536.
3. Zheng, J.; Lyu, Y.; Qiao, M.; Wang, R.; Zhou, Y.; Li, H.; Chen, C.; Li, Y.; Zhou, H.; Jiang, S. P.; Wang, S., Photoelectrochemical synthesis of ammonia on the aerophilic-hydrophilic heterostructure with 37.8% efficiency. *Chem.* **2019,** *5* (3), 617-633.
4. Zhang, Q.; Hu, S.; Fan, Z.; Liu, D.; Zhao, Y.; Ma, H.; Li, F., Preparation of g-C_3N_4/ZnMoCdS hybrid heterojunction catalyst with outstanding nitrogen photofixation performance under visible light via hydrothermal post-treatment. *Dalton T.* **2016,** *45* (8), 3497-3505.
5. Zhao, S.; Liu, H.-X.; Qiu, Y.; Liu, S.-Q.; Diao, J.-X.; Chang, C.-R.; Si, R.; Guo, X.-H., An oxygen vacancy-rich two-dimensional Au/TiO_2 hybrid for synergistically enhanced electrochemical N2 activation and reduction. *J. Mater. Chem. A* **2020,** *8* (14), 6586-6596.